Journal of Engineering Physics and Thermophysics, Vol. 65, No. 2, 1993

NUMERICAL INVESTIGATION OF THE EFFECT OF THE RADIATIVE PROPERTIES OF A TUBE WATERWALL AND COMBUSTION PRODUCTS ON HEAT TRANSFER IN TUBE FURNACES

A. M. Abdullin and D. V. Vafin

UDC 536.3:535.34

Heat transfer in the radiant section of a tube furnace is investigated within the framework of a mathematical model proposed in [1]. Results of calculations showing the effect of the tube waterwall emissivity and the partial pressure of H_2O and CO_2 in the composition of the combustion products on heat transfer are given.

Investigating the laws of combined heat transfer in tube furnaces is of great interest for ensuring their reliability and establishing additional possibilities on optimizing the operating conditions for these units. A radiative component whose share can be more than 90% is predominant in the heat balance of tube furnaces [1]. Therefore the accuracy of a thermal calculation of the furnaces is largely determined by the correctness of the model of radiative heat transfer and, in particular, by the correspondence of the radiative properties of the reaction tubes and the furnace space, prescribed as the initial data, to their real values. However, oxidation of the reaction tubes occurs in tube furnace operation, which results in a change in their radiative properties. Replacement of one fuel gas by another, a change in the excess-air coefficient, and other regime and structural changes may lead to a corresponding change in the radiative properties of the combustion products. Therefore, investigating the influence of the above factors on heat transfer in furnaces takes on great significance.

The object of the investigation is the radiant section of a tube furnace for conversion of a hydrocarbon gas, bounded by rows of vertically arranged tubes (Fig. 1). The reaction mixture enters the tubes from above and moves in the same direction as the combustion products. On the furnace arch a series of gas-burner devices is symmetrically arranged about tube waterwalls. On the furnace bottom there are smoke-removing ducts, by which the combustion products are carried off into the convection chamber.

A uniformly distributed regime of heat transfer is realized in the radiant section of this structure. This regime is characterized by the fact that the tube waterwall is not affected by the flame directly. The tube waterwall and the flame are separated by a region with the relatively lower temperature of the combustion products. Here, the recirculating turbulent character of the flow of the combustion products, the flame length, the process of fuel burn-out, and the selectivity of the radiation of the combustion products have a substantial effect on the heat transfer.

The small width of the radiant section as compared to its length and height and the symmetric arrangement of the gas-burner devices enable us to consider the heat transfer and the flow of gases in a cross section as a two-dimensional problem. In [2] it is shown that, when a gaseous fuel is burned, the effect of radiation scattering in the furnace volume can be ignored; hence, the equation of radiation transfer has the form

$$\mu \frac{\partial I_{s,k}}{\partial x} + \xi \frac{\partial I_{s,k}}{\partial y} = \frac{\alpha_k}{\Delta\lambda_k} \int_{\lambda_{k-1}}^{\lambda_k} J_{\lambda b}(\lambda,\ T)\, d\lambda - \alpha_k I_{s,k}, \quad k = 1,\ N. \tag{1}$$

The boundary condition to Eq. (1) with diffuse radiation and reflection from the walls is written as

$$I_{s,k} = \frac{\varepsilon}{\Delta\lambda_k} \int_{\lambda_{k-1}}^{\lambda_k} J_{\lambda b}(\lambda,\ T_w)\, d\lambda + \frac{r}{\pi} \int_{(s'n)<0} I_{s',k} \cos(s'n)\, d\omega_{s'} \tag{2}$$

for directions s such that (sn) > 0.

Kazan' Chemical Engineering Institute, Nizhnekamsk Branch. Translated from Inzhenerno-Fizicheskii Zhurnal, Vol. 65, No. 2, pp. 171-177, August, 1993. Original article submitted April 6, 1992.

 1062-0125/93/6502-0752$12.50

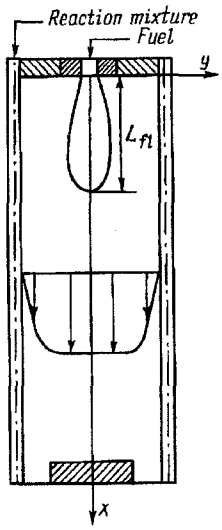

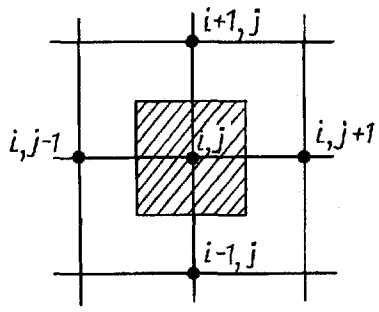

Fig. 1. Diagram of the radiant section and the coordinate system.

Fig. 2. Finite-difference grid.

The temperature field in the radiant section volume is determined from the energy conservation equation

$$c_p\rho\left[u\frac{\partial T}{\partial x}+v\frac{\partial T}{\partial y}\right]=\frac{\partial}{\partial x}\left[(\lambda+\lambda_T)\frac{\partial T}{\partial x}\right]+ \\ +\frac{\partial}{\partial y}\left[(\lambda+\lambda_T)\frac{\partial T}{\partial y}\right]+Q_v-\operatorname{div}\mathbf{q}_p. \tag{3}$$

Equation (3) should be supplemented with boundary conditions. The tube waterwall is conventionally replaced by a beam-absorbing surface, impermeable to matter, on which a reaction tube temperature characterizing the tube furnaces considered is prescribed. On the burner cut we prescribe the fuel mixture temperature calculated from the initial temperatures of the fuel and the air supplied for combustion, the excess-air coefficient, the portion of burnt fuel, and other parameters. The lining temperature is determined from the condition of its adiabatic nature, which has the form

$$\alpha_{con}(T-T_w)=[(\mathbf{q}_p\mathbf{n})]_w. \tag{4}$$

The fields of the velocity of motion for the combustion products and of the turbulent thermal conductivity coefficient are determined by a numerical solution of the time-averaged Navier-Stokes, continuity, and (k–ε) turbulence model equations [1]. The volume density of the heat release in the flame volume is calculated using the formula

$$Q_v=B_f Q_p^l\Delta\eta,$$

where $\Delta\eta$ is the change in the integral power of fuel burn-out between the two considered cross sections of the flame. The integral power of fuel burn-out is prescribed by the semiempirical dependence [3]

$$\eta(x)=1-\exp\left[-a\left(\frac{x}{L_{fl}}\right)^2\right].$$

Radiative heat transfer is dealt with in the S_2 approximation of a discrete ordinate method. Within the framework of this method Eq. (1) is approximated by the system of differential equations relative to radiation intensities along four selected directions:

$$\mu_m\frac{\partial I_{m,k}}{\partial x}+\xi_m\frac{\partial I_{m,k}}{\partial y}=\frac{\alpha_k}{\Delta\lambda_k}\int_{\lambda_{k-1}}^{\lambda_k}J_{\lambda b}(\lambda,\ T)\,d\lambda-\alpha_k I_{m,k}. \tag{5}$$

Each direction is prescribed by the angular coordinates $\{\mu_m, \xi_m; m = 1, 4\}$.

Condition (2) on the boundary x = const is approximated as:

$$I_{m,k} = \frac{\varepsilon}{\Delta\lambda_k} \int_{\lambda_{k-1}}^{\lambda_k} J_{\lambda b}(\lambda, T_w)\, d\lambda + \frac{r}{\pi} \sum_{m'=1}^{4} w_{m'} |\mu_{m'}| I_{m',k}. \tag{6}$$

On the boundary x = 0 we have $\mu_m > 0$, $\mu_{m'} < 0$; on the boundary x = L we have $\mu_m > 0$, $\mu_{m'} > 0$. On the boundary y = const there is a uniqueness condition analogous to (6). The set of angular coordinates μ_m, ξ_m and weight factors w_m was prescribed from the data of [4].

The system of equations (3) and (5) with the corresponding boundary conditions is solved numerically on a nonuniform finite-difference grid. Integrating Eq. (5) over the cross-hatched area element (Fig. 2) gives its discrete analog:

$$\mu_m A_j (I^{i+1,j}_{m,k} - I^{i-1,j}_{m,k}) + \xi_m B_i (I^{i,j+1}_{m,k} - I^{i,j-1}_{m,k}) = 4\alpha^k_{i,j} A_j B_i (R^k_{i,j} - I^{i,j}_{m,k}), \tag{7}$$

where

$$A_j = \frac{1}{2}(y_{j+1} - y_j); \quad B_i = \frac{1}{2}(x_{i+1} - x_i); \quad R^k_{i,j} = \frac{1}{\Delta\lambda_k} \int_{\lambda_{k-1}}^{\lambda_k} J_{\lambda b}(\lambda, T_{i,j})\, d\lambda.$$

We consider the case $\mu_m > 0$, $\xi_m > 0$. If the radiation intensity is a smoothly varying function of coordinates, $I^{i,j}_{m,k}$ can be approximately represented as

$$I^{i,j}_{m,k} = \omega I^{i,j+1}_{m,k} + (1 - \omega) I^{i,j-1}_{m,k} = \omega I^{i+1,j}_{m,k} + (1 - \omega) I^{i-1,j}_{m,k}, \tag{8}$$

where ω is the interpolation coefficient. Substituting (8) into Eq. (7) and performing manipulations, we obtain the recurrence formula

$$I^{i,j}_{m,k} = \frac{\mu_m A_j I^{i-1,j}_{m,k} + \xi_m B_i I^{i,j-1}_{m,k} + 4\omega\alpha^k_{i,j} A_j B_i R^k_{i,j}}{\mu_m A_j + \xi_m B_i + 4\omega\alpha^k_{i,j} A_j B_i}. \tag{9}$$

For negative values of μ_m and ξ_m formulas analogous to (9) can be obtained.

The system of algebraic equations (7) is solved by a method of coordinate run which can be expressed by the following iteration scheme:

1) the initial approximation for the radiation intensity $I^{i,j}_{m,k}$ is prescribed;

2) using Eq. (6) the radiation intensity $I^{i,j}_{m,k}$ is calculated on the boundary surfaces for m = 1, 4 and k = 1, N;

3) using formula (9) $I^{i,j}_{m,k}$ is calculated at all points of the finite-difference grid for m = 1, 4 and k = 1, N;

4) the calculated radiation intensity field $I^{i,j}_{m,k}$ is taken for the initial approximation;

5) beginning with par. 2, the calculation procedure is repeated until convergent solution is obtained.

Similarly we can obtain the discrete analog of the energy conservation equation (3):

$$p_{i,j} T_{i,j} - a_{i,j} T_{i+1,j} - c_{i,j} T_{i-1,j} - b_{i,j} T_{i,j+1} - d_{i,j} T_{i,j-1} = f_{i,j}, \tag{10}$$

where

$$p_{i,j} = a_{i,j} + c_{i,j} + b_{i,j} + d_{i,j} + \frac{1}{4}(S_p)_{i,j}(x_{i+1} - x_{i-1})(y_{j+1} - y_{j-1});$$

$$f_{i,j} = \frac{1}{4}(S_c)_{i,j}(x_{i+1} - x_{i-1})(y_{j+1} - y_{j-1});$$

$a_{i,j}$, $c_{i,j}$, $b_{i,j}$, and $d_{i,j}$ are the known coefficients [5]. To ensure stability of the calculation algorithm, the source term in the energy equation is represented in a linearized form:

$$S_f = Q_v - \operatorname{div} \mathbf{q}_p = S_c - S_p T.$$

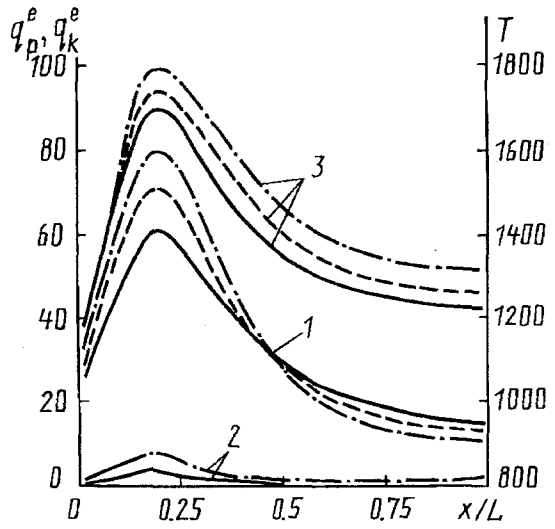

Fig. 3. Radiative (1) and convective (2) heat flux density distribution and the temperature profile (3) along the radiant section height; solid curves) $\varepsilon = 1$; dashed curves) 0.7; dot-dash curves) 0.5. q^e_p, q^e_k, kW; T, K.

If we express div q_p in terms of the radiation intensity, we can obtain the following expressions for S_c and S_p:

$$S_c = Q_v + \sum_{k=1}^{N} \alpha_k \sum_{m=1}^{4} w_m I_{m,k} \Delta\lambda_k; \quad S_p = \frac{1}{T^*} \sum_{k=1}^{N} \alpha_k \int_{\lambda_{k-1}}^{\lambda_k} J_{\lambda b}(\lambda, T)\, d\lambda,$$

where T^* is the combustion product temperature calculated at the previous iteration step.

The system of algebraic equations (10) with the corresponding uniqueness conditions is solved by the iteration linear method with the tridiagonal matrix algorithm [5]. Simultaneous solution of the system of differential equations (3) and (5) with the boundary conditions (4) and (6) is performed by a method of successive approximations. We emphasize that the radiation intensity $I_{m,k}$ and the combustion product temperature T are determined at the same points of the finite-difference grid. This being so, the most correct agreement of the method for calculating radiative heat transfer with the gasdynamic part of the problem is attained.

A numerical investigation of the effect of the tube waterwall emissivity on the density distribution of radiative and convective heat fluxes to the tube waterwall and the temperature profile of combustion products along the height of the tube furnace radiant section was performed (see Fig. 1). It was assumed that the radiant section volume is filled with the complete combustion products of natural gas: H_2O, CO_2, N_2, and O_2. The presence of O_2 is caused by the excess of air supplied to the burners (the excess-air coefficient is $\alpha_f = 1.1$). The flame length is $L_{fl} = 4$ m [6]. The radiation spectrum of the combustion products is described by the wide-band model, taking account of bands of 1.5, 2.7, 6.3, and 10 μm of the radiation spectrum of H_2O and those of 2.7, 4.3, and 15 μm of CO_2. The dependence of the thermophysical and radiative properties of combustion products on the temperature was taken into account in the calculations. The interpolation coefficient ω in Eq. (8) was assumed equal to 0.5.

Figure 3 gives the calculated distribution of densities for the radiative and convective heat fluxes to the tube waterwall and the temperature profile of the combustion products along the radiant section height with $\varepsilon = 0.5$, 0.7, 1.0. The tube waterwall emissivity has a significant influence on the temperature and heat flux fields in the radiant section. The portion of the radiation reflected from the tube waterwall that is absorbed by the combustion products and goes for increasing their internal energy increases with decreasing ε. Because of this an increase in the combustion product temperature is observed throughout the entire volume of the radiant section. In particular, when the tube waterwall emissivity changes from 1.0 to 0.5, the maximum temperature of the combustion products in the flame region increases by 90°C. As a consequence an increase in the convective heat flux to the tube waterwall is observed, which, for small values of ε, largely compensates a decrease in the radiative heat flux to the tube waterwall. However, the emissivity of the tube waterwall has the greatest effect on the value of the total (radiation plus convection) heat flux for values smaller than 0.6 (Fig. 4). In the region $0.6 < \varepsilon < 1$ characterizing real units this effect does not exceed

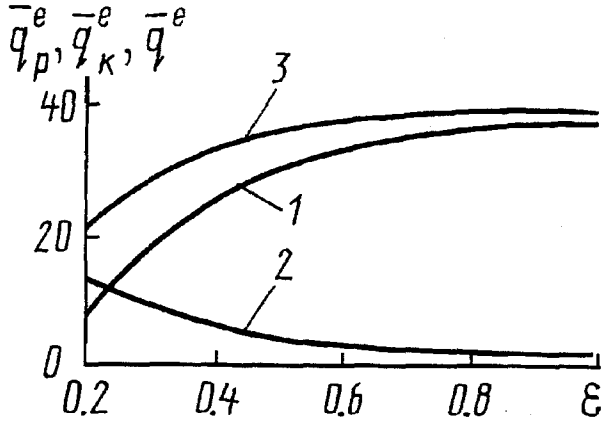

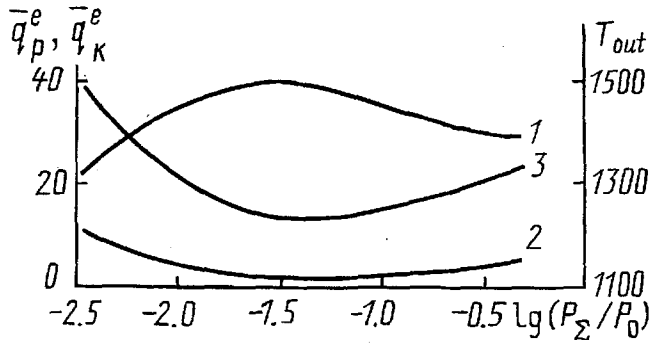

Fig. 4. Dependence of the average densities of the radiative (1), convective (2), and total (3) heat fluxes to the tube waterwall on ε.

Fig. 5. Dependence of the average densities of the radiative (1) and convective (2) heat fluxes and the gas temperature at the outlet from the furnace (3) on P_Σ; $P_0 = 1$ atm.

5%. With increasing ε the degree of heating nonuniformity for the reaction tubes along their length also increases. Whereas with an increase in the tube waterwall emissivity from 0.5 to 1.0 the average density of the total heat flux increases by 8%, its maximum value in the flame region increases by 18%.

The tube waterwall emissivity does not have a unique effect on the local values of the radiative heat flux density q^e_p. The intrinsic radiation of the tube waterwall is small due to its relatively low temperature, and therefore the resultant radiative heat flux to the tube waterwall mainly depends on its emissivity and value of the incident radiative flux. Intensive cooling of the flame with large values of ε downstream leads to a decrease in the radiative heat flux incident on the tube waterwall. As a result, the density of the radiative heat flux to the tube waterwall increases with increasing ε in the flame region, and downstream the reverse picture is observed: a higher density of the radiative heat flux to the tube waterwall corresponds to smaller ε values.

The effect of the partial pressure of emitting components in the composition of the combustion products on the characteristics of local and overall heat transfer in the radiant section of the tube furnace considered in the present work was also investigated numerically. In the calculations the ratio of the partial pressure of water vapor P_w to that of carbon dioxide P_c was maintained equal to 2 and their total partial pressure P_Σ was varied from 0 to 0.48 atm. Since the absorption factor of combustion products depends on the partial pressures of H_2O and C_2O in direct proportion, the investigation under consideration can also be considered from the viewpoint of the effect of the optical density of the furnace volume on radiative-convective heat transfer.

A very peculiar effect of P_Σ on the value of the radiative heat flux to the tube waterwall is found. The intensity of heat transfer between the tube waterwall and the combustion products is affected by two interrelated factors. As the partial pressure of the emitting components increases, the emissivity of the furnace volume increases, which causes an increase in its intrinsic radiation. The second factor involves an increase in the optical density and a decrease in the transparency of the furnace medium, which leads to a diminished role of the high-temperature region of the flame in forming the radiative heat flux to the tube waterwall. As Fig. 5 shows, in the region $P_\Sigma < 0.03$ atm the factor of screening of the flame due to the sufficiently high transparency of the furnace medium does not have a substantial effect on the conditions of heat transfer, and therefore with increasing P_Σ the radiative heat flux to the tube waterwall increases. When P_Σ increases further, a radiative heat transfer maximum is attained, and then the radiative heat flux to the tube waterwall decreases somewhat. This is explained by the low optical transparency of the furnace medium with relatively large values of the partial pressure of emitting components in the composition of the combustion products.

Thus, it is established that for a given width of the radiant section an optimum partial pressure exists for the emitting components in the composition of the combustion products (or optical density of the furnace volume), ensuring maximum heat transfer to the tube waterwall. At the same time we emphasize that the value $P_\Sigma = 0.27$ atm

characterizing real operation of tube furnaces is approximately an order of magnitude larger than the optimum value from the viewpoint of maximum heat transfer.

NOTATION

x, y, coordinates; $I_{s,k}$, intensity of the integral radiation in the spectral interval $[\lambda_{k-1}, \lambda_k]$ in the direction s; α_k, integral absorption factor over the k-th spectral band; $\Delta\lambda_k = \lambda_k - \lambda_{k-1}$; $J_{\lambda b}$, Planck function; N, number of spectral bands; T, temperature; ε, emissivity; r, reflectivity; n, internal normal; c_p, heat capacity; ρ, density; u, v, velocity vector components; λ, λ_T, molecular and turbulent thermal conductivity coefficients, respectively; q_p, radiation heat flux density vector; α_{con}, convective heat transfer coefficient; B_f, fuel rate; Q_p^l, lower heat value of fuel; a, empirical coefficient; L_{fl}, flame length; q_p^e, q_k^e, q^e, densities of radiant, convective, and total heat fluxes to the tube waterwall; $\bar{q}_p^e$, $\bar{q}_k^e$, $\bar{q}^e$, values of q_p^e, q_k^e, q^e averaged over the tube length; T_{out}, gas temperature at the outlet from the radiant section; L, radiant section height. Subscripts: w, value on the boundary; m, value along the direction (μ_m, ξ_m); k, value in the k-th spectral band; i, j, value at the nodal point with the coordinates x_i, y_j.

REFERENCES

1. A. M. Abdullin and D. B. Vafin, Inzh. Fiz.-Zh., **60**, No. 2, 291-297 (1991).
2. A. G. Blokh, Heat Transfer in Steam Boiler Furnaces [in Russian], Leningrad (1984).
3. V. G. Lisienko, Intensification of Heat Transfer in Combustion Furnaces [in Russian], Moscow (1979).
4. J. S. Truelove, Trans. ASME: J. Heat Transfer, **109**, No. 4, 1048-1051 (1987).
5. S. Patankar, Numerical Methods for Solving Problems of Heat Transfer and Fluid Dynamics [Russian translation], Moscow (1984).
6. B. M. Krivonogov, Increasing the Efficiency of Burning of Gas and Environmental Protection [in Russian], Leningrad (1986).